Crystallization of Malonic and Succinic Acids on SAMs: Toward the General Mechanism of Oriented Nucleation on Organic Monolayers[†]

Boaz Pokroy,[‡] Victoria Fay Chernow, and Joanna Aizenberg*

School of Engineering and Applied Sciences, Department of Chemistry and Chemical Biology, Harvard University, Cambridge, Massachusetts 02138. [‡] Current address: Department of Materials Engineering, Israel Institute of Technology, Haifa 32000, Israel.

Self-assembled monolayers (SAMs) were shown to induce very specific oriented growth of simple organic and inorganic crystals. Here we present a detailed study of the mechanism by which SAMs control the oriented nucleation by examining a more complex case of crystallization of bifunctional organic molecules. Malonic and succinic acids were grown on the SAMs of $HS(CH_2)_{10}CO_2H$ and $HS(CH_2)_{11}CO_2H$ supported on gold films. Each SAM induced a very controlled, specific orientation of the crystals. The preferred nucleating planes always exhibited an alignment of one of the carboxylic acid groups in the molecules of the growing crystal with the carboxylic acid groups on the surface of the SAMs. These results suggest that the translation of the structural information through the interface occurs by stereochemical registry such that the functional groups in the SAM play the role of an oriented surrogate layer for the nucleating crystal. These findings are very important to the understanding of the underlying principles by which various organic surfaces—and most probably also biological templates—control the crystallization process.

Introduction

An understanding of crystal nucleation and growth and the ability to control the crystallization process are extremely important in many aspects of science and technology.[1] This control is usually achieved by the use of inorganic crystalline substrates that induce nucleation via epitaxy.[2] Successful crystallization on these substrates is dependent on the ability to engineer the interface that provides a good lattice match between the substrate and a certain crystallographic plane of the overgrowing crystalline material. For this purpose, much effort is invested in the development of new, low-mismatch epitaxial inorganic materials that direct the growth of the nascent crystalline phase in specific crystallographic orientations and thus control the optical, electronic, mechanical, biochemical, and catalytic properties. However, the high symmetries of the surfaces in the substrate inorganic crystals put severe limitations on the resulting crystal orientations, especially when symmetry breaking is required to ensure the nucleation and stabilization of a low-symmetry phase and its growth in an arbitrary crystallographic direction.[3]

The formation of a variety of crystalline materials in organisms, however, is templated by bioorganic substrates that exert very high control over crystal nucleation and growth, including polymorph selection, crystallographic orientation, defect distribution, and patterning.[4] In the materials community, there is a growing appreciation of the potential of biomimetic approaches to crystallization when organic surfaces are used as crystallization templates to control the formation of both organic and inorganic materials. Several types of biomimetic structured organic substrates have been employed for such purposes. Prominent examples include organic monolayers such as Langmuir monolayers[5,6] and self-assembled monolayers (SAMs).[7−15] Alkanethiol-based SAMs are known to form very ordered 2D crystals on coinage metals.[16,17] These SAM organizations have been well characterized in terms of their 2D lattice and the tilt and cant angles of the alkyl chains.[18−22] The lattice parameters of the surface can be controlled to a certain extent by choosing the appropriate thiol/metal combination. In addition, the use of ω-functionalized SAMs allows for fine-tuning the surface chemistry, charge, polarity, and orientation of the terminal groups. These SAMs have been shown to be extremely potent in inducing the

(5) Landau, E. M.; Popovitz-biro, R.; Levanon, M.; Leiserowitz, L.; Lahav, M.; Sagiv, J. *Mol. Cryst. Liq. Cryst.* **1986**, *134*, 323–335.
(6) Arkadi, L. L.; Suresh, V.; David, L. K.; Stephen, M. *Adv. Mater.* **1997**, *9*, 124–127.
(7) Flath, J.; Meldrum, F. C.; Knoll, W. *Thin Solid Films* **1998**, *329*, 506–509.
(8) Meldrum, F. C.; Flath, J.; Knoll, W. *J. Mater. Chem.* **1999**, *9*, 711–723.
(9) Heywood, B. R.; Mann, S. *Adv. Mater.* **1994**, *6*, 9–20.
(10) Aizenberg, J.; Black, A. J.; Whitesides, G. M. *J. Am. Chem. Soc.* **1999**, *121*, 4500–4509.
(11) Aizenberg, J.; Black, A. J.; Whitesides, G. M. *Nature* **1999**, *398*, 495–498.
(12) Han, Y. J.; Aizenberg, J. *Angew. Chem., Int. Ed.* **2003**, *42*, 3668–3670.
(13) Briseno, A. L.; Aizenberg, J.; Han, Y. J.; Penkala, R. A.; Moon, H.; Lovinger, A. J.; Kloc, C.; Bao, Z. A. *J. Am. Chem. Soc.* **2005**, *127*, 12164–12165.
(14) Dabros, M.; Thalladi, V. R. *Chem. Commun.* **2007**, *24*, 2476–2478.
(15) Cox, J. R.; Dabros, M.; Shaffer, J. A.; Thalladi, V. R. *Angew. Chem., Int. Ed.* **2007**, *46*, 1988–1991.
(16) Ulman, A. *An Introduction to Ultrathin Organic Films: From Langmuir−Blodgett to Self - Assembly*; Academic Press: San Diego, CA, 1991.
(17) Love, J. C.; Estroff, L. A.; Kriebel, J. K.; Nuzzo, R. G.; Whitesides, G. M. *Chem. Rev.* **2005**, *105*, 1103–1169.
(18) Laibinis, P. E.; Whitesides, G. M. *J. Am. Chem. Soc.* **1992**, *114*, 1990–1995.
(19) Nuzzo, R. G.; Dubois, L. H.; Allara, D. L. *J. Am. Chem. Soc.* **1990**, *112*, 558–569.
(20) Fenter, P.; Eisenberger, P.; Liang, K. S. *Phys. Rev. Lett.* **1993**, *70*, 2447–2450.
(21) Chaudhuri, A.; Lerotholi, T. J.; Jackson, D. C.; Woodruff, D. P.; Robert, G. J. *Phys. Rev. B* **2009**, *79*, 195439.
(22) Fang-Sen, L.; Wancheng, Z.; Quanmin, G. *Phys. Rev. B* **2009**, *79*, 113412.

(1) Scheel, H. J.; Capper, P., Eds.; *Crystal Growth Technology: From Fundamentals and Simulation to Large-Scale Production*; Wiley-VCH: Weinheim, Germany, 2008; p 505.
(2) Herman, M. A.; Richter, W.; Sitter, H. *Epitaxy: Physical Principles and Technical Implementation*; Springer-Verlag: Berlin, Germany, 2004; p 522.
(3) Georgakilas, A.; Panayotatos, P.; Stoemenos, J.; Mourrain, J. L.; Christou, A. *J. Appl. Phys.* **1992**, *71*, 2679–2701.
(4) Lowenstam, H. A.; Weiner, S. *On Biomineralization*; Oxford University Press: New York, 1989.

very specific oriented nucleation of a variety of crystalline materials.[7−15]

We have previously proposed that the orientation in these systems is not governed by the epitaxial match between the lattices of the SAM and the crystal nucleation plane, as observed in the traditional inorganic substrates, but rather by their stereochemical registry[10,12,13]—a spatial match between the orientation of the SAM's functional groups and that of a certain moiety (or ion) in the nucleated crystal. This mechanism was demonstrated to operate in templating the oriented growth of both inorganic and organic crystals. In particular, the growth of calcium carbonate on carboxylate-terminated SAMs was shown to favor calcite orientations with a perfect stereomatch and alignment of the carboxylates in the SAM with the carbonates in calcite, with highly mismatched lattices.[10,12] Similarly, anthracene crystals grown on terphenylthiol SAMs exhibited preferred orientation with anthracene molecules coaligned with the terphenyl groups in the SAM,[13] even though such an orientation leads to a lattice mismatch at the interface.[23]

Here we study the generality of the proposed mechanism of oriented nucleation at organic surfaces by examining a more complex case of crystallization of bifunctional organic molecules. The importance of understanding the crystallization of such systems arises from the fact that the molecules in the nascent crystalline phase can present more than one orientational match with the interface or more than one matching group, thus allowing one to observe how the system selects or discriminates certain orientations and to derive the underlying basic principles. To this end, we have chosen to study the SAMs-induced crystallization of two carboxylic diacids—malonic acid (HOO-CCH$_2$COOH) and succinic acid (HOOCCH$_2$CH$_2$COOH). Malonic acid exhibits a triclinic unit cell with the $P1$ space group ($a = 5.330$ Å, $b = 5.140$ Å, $c = 11.250$ Å, $\alpha = 70°$, $\beta = 135.17°$, and $\gamma = 85.17°$).[24] Succinic acid exhibits a monoclinic unit cell with the $P2_1/c$ space group ($a = 5.526$ Å, $b = 8.881$ Å, $c = 5.105$ Å, and $\beta = 91.49°$).[25] Both acids have two molecules per unit cell, thus presenting four different orientations of the carboxylic acid groups in the crystalline state. We show that in these complex systems the SAMs induce very controlled oriented growth of the crystals. The preferred nucleating planes always exhibit an alignment of one of the carboxylic acid groups in the molecules of the growing crystal with the carboxylic acid groups on the surface of the SAMs. These results further confirm that the translation of structural information through the organic interface occurs by stereochemical registry such that the functional endgroups in the SAM play the role of an oriented surrogate layer for the nucleating crystal.

Results and Discussion

When choosing the organic substrates, we took advantage of the well-known odd−even effect in SAMs[26] supported on gold; that is, the terminal groups of the ω-functionalized SAMs are oriented differently at the interface depending on the parity of the alkyl chain, and the 2D lattice symmetry and spacing in the monolayer are identical. In particular, by using the known structural information regarding the cant (α) and twist (β) angles of these monolayers on Au(111) ($|\alpha| = 26−28°$, $|\beta| = 50−55°$),[27]
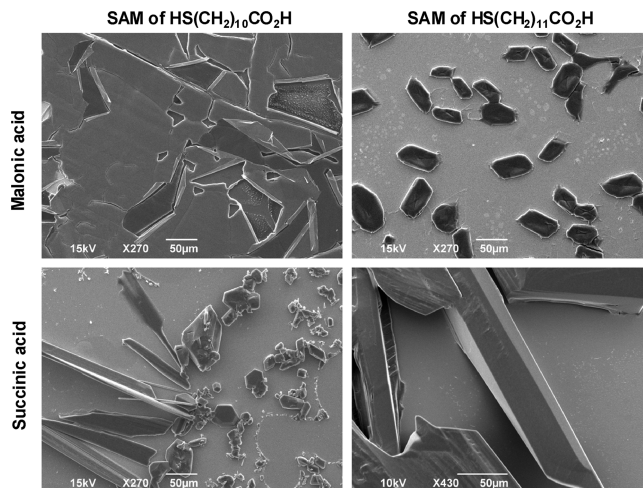

Figure 1. SEM images of the crystals of malonic (top) and succinic (bottom) acids grown on the SAMs of HS(CH$_2$)$_{10}$CO$_2$H (left) and HS(CH$_2$)$_{11}$CO$_2$H (right) supported on gold.

we can calculate that the angle between the surface normal and the C−X bond (the bond between the terminal group X and the last carbon atom in the alkyl chain) is equal to $20° \pm 3°$ and $52° \pm 3°$ for the SAMs with an even and odd number of methylene groups, respectively. Such a significant difference makes these SAMs ideal substrates for studies of the effects of orientation and stereochemical recognition at the interface. It has been shown that odd and even SAMs induce different, specific orientations of crystals[12,28] as well as polymorph selectivity.[14,15]

Succinic and malonic acids were allowed to crystallize on SAMs of HS(CH$_2$)$_{10}$CO$_2$H and HS(CH$_2$)$_{11}$CO$_2$H supported on gold films. Each surface induced the formation of a characteristic, morphologically distinct crystalline phase for the odd and even SAMs (Figure 1). The XRD analysis revealed a significant increase in the intensity of certain system-specific peaks, as compared to the diffraction patterns of the randomly oriented powder samples of the crystals of succinic and malonic acids (Figure 2).

The preferred nucleating planes were determined using the March−Dollase method.[29] In this approach, a single parameter is calculated, $r = \left(\dfrac{\sin^2 \alpha}{(k/k_{\mathrm{p}})^{2/3} - \cos^2 \alpha} \right)^{1/3}$, $0 \leq r \leq 1$ where α is the angle between the plane of preferred orientation and the comparison plane and k and k_{p} are the observed and random powder intensity ratios between the two planes under consideration, respectively. In general, as a comparison one can use any desired plane as long as it has a detectable diffraction peak. However, to get better accuracy one should attempt to choose a plane that forms the smallest angle with the plane of investigation. A perfect uniaxial preferred orientation will give $r = 0$, and a randomly oriented powder will give $r = 1$. Using a recent extension of this approach, one can estimate the degree of preferred orientation:[30]

$$\eta = 100\%[(1-r)^3/(1-r^3)]^{1/2}.$$

Crystals of malonic acid grown on HS(CH$_2$)$_{11}$CO$_2$H exhibited essentially one preferred nucleating plane—the (10-2) with $\eta = 94\%$. When malonic acid was grown on HS(CH$_2$)$_{10}$CO$_2$H, it

(23) Pokroy, B.; Aizenberg, J. *CrystEngComm* **2007**, *9*, 1219–1225.
(24) Goedkoop, J. A.; Macgillavry, C. H. *Acta Crystallogr.* **1957**, *10*, 125–127.
(25) Thalladi, V. R.; Nusse, M.; Boese, R. *J. Am. Chem. Soc.* **2000**, *122*, 9227–9236.
(26) Tao, F.; Bernasek, S. L. *Chem. Rev.* **2007**, *107*, 1408–1453.
(27) Laibinis, P. E.; Nuzzo, R. G.; Whitesides, G. M. *J. Phys. Chem.* **1992**, *96*, 5097–5105.

(28) Knoesen, A.; Pakalnis, S.; Follonier, S.; Miller, W.; Abbott, N.; Lee, N.; Frank, C. *Annu. Meet. IEEE, 14th* **2001**, *2*, 632–633.
(29) Dollase, W. A. *J. Appl. Crystallogr.* **1986**, *19*, 267–272.
(30) Zolotoyabko, E. *J. Appl. Crystallogr.* **2009**, *42*, 513–518.
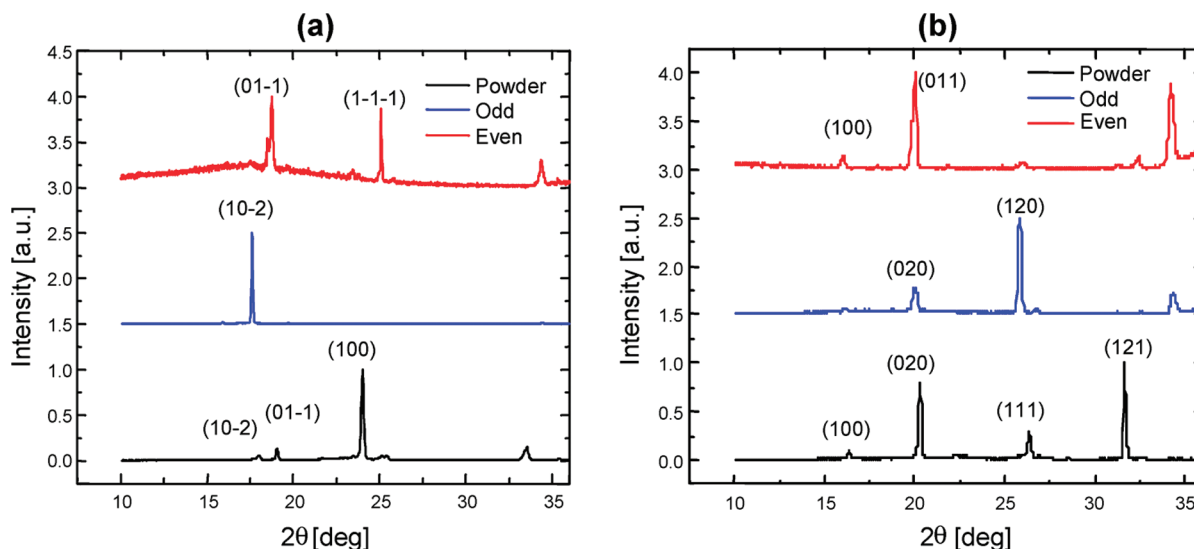
Figure 2. Powder X-ray diffraction spectra of malonic (a) and succinic (b) acids grown on the SAMs of $HS(CH_2)_{10}CO_2H$ and $HS-(CH_2)_{11}CO_2H$ supported on gold films. Each case is compared to the powder diffraction pattern of randomly oriented powder samples. Pronounced preferred orientations are observed in all cases.

Table 1. Structural Parameters Describing the Preferred Crystallographic Orientations of Malonic and Succinic Acids Grown on Self-Assembled Monolayers[a]

crystal	monolayer	nucleating plane	η (%)	r	ζ_1 (deg)	ζ_2 (deg)
malonic acid	$HS(CH_2)_{10}CO_2H$ on Au(111)	(01-1)	45	0.237	0−3	6−11
		(10-1)	13	0.518	4−9	40−45
		(010)	10	0.566	11−16	30−35
		(1-1-1)	6	0.648	11−16	40−48
	$HS(CH_2)_{11}CO_2H$ on Au(111)	(10-2)	94	0.020	0−5	20−24
succinic acid	$HS(CH_2)_{10}CO_2H$ on Au(111)	(011)	51	0.200	0−3	33−38
		(020)	23	0.400	6−11	12−17
		(100)	14	0.504	14−19	14−19
		(111)	5	0.674	16−21	61−66
	$HS(CH_2)_{11}CO_2H$ on Au(111)	(120)	56	0.179	2−7	38−43
		(020)	9	0.584	6−11	12−17

^{a} η is the degree of preferred orientation,[30] r is the March−Dollase parameter,[29] and ζ is the stereochemical mismatch parameter (see the text for details).

revealed primarily the (01-1) nucleating plane ($\eta = 45\%$) and three additional orientations—(10-1), (100), and (1-1-1) with $\eta = 13, 10,$ and 6%, respectively. Succinic acid grown on $HS(CH_2)_{11}CO_2H$ exhibited mostly the (120) nucleating plane ($\eta = 56\%$) and the (020) secondary plane ($\eta = 9\%$). When it was grown on $HS(CH_2)_{10}CO_2H$, it revealed primarily the (011) nucleating plane ($\eta = 51\%$) and three secondary orientations—(020), (100), and (111) with $\eta = 23, 14,$ and 5%, respectively (Table 1). In control experiments, the crystals were grown on bare (110) Si wafers. These crystals showed no preferred orientation (Supporting Information).

When considering the XRD orientation analysis, it is important to bear in mind that in the conventional Bragg−Brentano configuration only surfaces parallel to the diffraction plane produce diffraction and this is so as long as that specific reflection is allowed by symmetry considerations. This means that one has to exercise great caution when dealing with the diffraction pattern because the apparent preferred orientation plane observed by XRD is not necessarily the actual plane with the highest preferred orientation. Therefore, the assignment of the nucleating planes based on the XRD is approximate and not straightforward. In particular, when the actual nucleation plane forms an angle of several degrees with the major plane observed in the XRD pattern, the latter will give a much lower diffraction intensity than the intensity that should be expected for the corresponding fraction of the oriented crystals. As a result, the degree of

preferred orientation calculated from the XRD is probably lower than the real value in most instances. To illustrate this point, let us consider, for example, the oriented growth of calcite on carboxylate-terminated SAMs supported on silver, as reported in ref 10. In this case, it was clear from the precise morphological analysis that the actual preferred nucleating plane forms an angle of ∼2° with the (012) plane observed in the XRD and that nearly 98% of calcite crystals showed this preferred orientation. However, when we analyze the X-ray data presented in the publication[10] using the same March parameter approach, we derive a degree of preferred orientation of $\eta = 51\%$ corresponding to a March−Dollase parameter of $r = 0.2$. (A detailed examination of the possible errors in the determination of the preferred orientations based on the XRD analysis is presented in the Supporting Information.)

These examples emphasize that for the unequivocal assignment of the preferred orientations it is important to perform a vis-à-vis morphological analysis, when possible. However, neither succinic acid nor malonic acid crystals grown on the SAM surfaces demonstrated clear facets (Figure 1) that could be used to determine their orientation morphologically, as in the case of calcite or anthracene.[10,12,13] Therefore, we could base our conclusions only on the XRD data. The analysis presented above, however, suggests that the observed primary preferred orientations with $\eta = 45, 94, 51,$ and 56% (Table 1) may, in reality, represent a very high (nearly 100%) degree of orientational
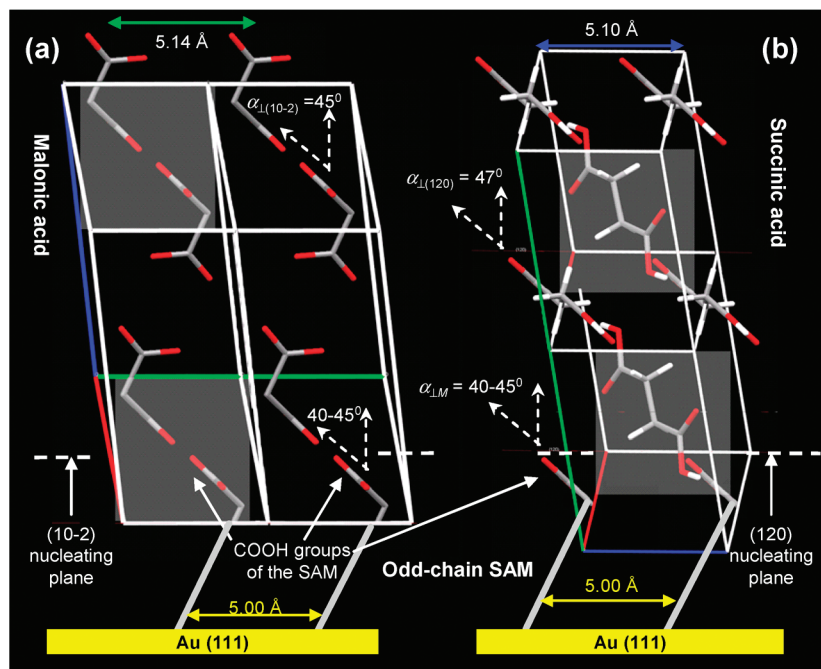
Figure 3. Superposition of the structures of oriented crystals and the underlying SAM of $HS(CH_2)_{11}CO_2H$ supported on Au(111). (a) Malonic acid preferentially nucleates from the (10-2) plane. (b) Succinic acid preferentially nucleates from the (120) plane. One of the carboxylic acid groups in each crystal in these orientations shows nearly absolute alignment with the carboxylic acid groups of the SAM. The interfacial motifs that involve the carboxylic groups from the SAM are therefore identical to the repeating motifs in the oriented crystal. (See the shaded areas.)

specificity, and the lower values may reflect the fact that the actual nucleating planes form a small angle with the apparent orientations observed in the XRD. Moreover, the supporting gold films deposited in our experiments by the PVD methods have a characteristic polycrystalline structure exhibiting a very strong (111) texture with a mean grain size of about 30 nm. The size of the single domains is much larger than the area required for a nucleation event to occur. Although accidental nucleation at the domain boundaries can also occur (which will reduce the degree of preferred orientation), the nucleating interface can be largely approximated by the structure of the SAM supported on the (111) Au surface. This will give rise to a fixed, primary nucleating plane of the growing crystals. The crystals will, however, have different in-plane orientations arising from the polycrystalline (111) domains and six symmetry-related orientations of the adsorbed SAMs.

To analyze the extent of stereochemical registry that occurs at the SAM−crystal interface, we compared the orientation of the carboxylic acid groups in the observed preferred nucleating planes of the malonic and succinic acids with those in the odd and even SAMs supported on Au(111). We define a general stereochemical mismatch parameter, ζ, between the orientations of the functional groups in the monolayer and those in the polyfunctional molecules of the growing crystal

$$\zeta_i = |(\alpha_{\perp(hkl)M} - \alpha_{\perp(hkl)C_i})|$$

where $\alpha_{\perp(hkl)M}$ is the angle that the plane of the functional groups in the monolayer forms with the surface normal and $\alpha_{\perp(hkl)C_i}$ is the angle that the plane of the *i*th functional group in the crystal forms with the normal to the (*hkl*) plane of preferred orientation. In our case, $\alpha_{\perp(hkl)M}$ is equal to $\sim17°−22°$ and $\sim40°−45°$ for the orientations of the carboxylic groups in the even and odd SAMs, respectively.[12] The parameters ζ for all preferential orientations observed for malonic and succinic acids grown on the SAMs are presented in Table 1. It shows a

nearly absolute alignment ($\zeta = 0−2°$) of one of the carboxylic acid groups in the crystals with the SAM for the primary nucleating planes. For the secondary nucleating planes, the extent of preferred orientation η decreases with the increase in ζ.

This information offers insight into why certain orientations are much more prominent than others and indicates that the stereochemical mismatch is a very important factor in determining the preferred orientation of crystal growth. This mismatch can be put side by side with the lattice mismatch parameter that is generally used to describe epitaxial crystal growth.[23] Our results suggest that the mechanism of oriented crystal growth of complex multifunctional organic molecules induced by the SAM is likely to be similar to that proposed for the crystallization of inorganic and simple organic molecules. In particular, the preferred nucleating planes exhibit the alignment of one of the carboxylic acid groups in the molecules of the growing crystal with the carboxylic acid groups on the surface of the SAMs. Once this orientation is fixed, the second molecule just follows the crystal structure and packing. This means that the interfacial motifs that involve the carboxylic groups from the SAM are identical to the repeating motifs in the oriented crystal.

To visualize the latter argument better, an example of selective nucleation of malonic and succinic acids on the SAMs of HS-$(CH_2)_{11}CO_2H$ is discussed in detail in Figure 3. One of the C−COOH bonds in the crystals of malonic acid forms an angle of 54° with the predominant (10-2) nucleating direction, and one of the C−COOH bonds in the crystals of succinic acid forms an angle of 55° with the predominant (120) nucleating direction. These bonds are, therefore, parallel to the C−COOH bonds in the SAM that form an angle of $\sim49−55°$ with the interface. Moreover, the planes of the aligned groups in malonic acid form an angle of $\alpha_{\perp(10-2)} = 45°$, and those in succinic acid form an angle of $\alpha_{\perp(120)} = 47°$, which correspond to $\zeta = 0$ and 2°, respectively. The interfacial orientation of these carboxylic acid groups in crystals
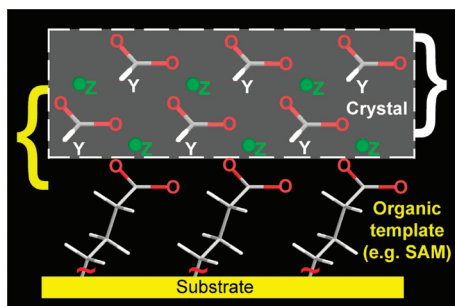
Figure 4. Schematic presentation depicting the proposed general mechanism of oriented crystallization induced by organic monolayers that involves the translation of stereochemical information through the interface (carboxylic acid-terminated SAMs shown as an example). The interfacial layer that includes functional groups of the monolayer and the co-oriented molecules of the nucleated crystal (yellow brace) is identical to the repeating layers of the crystal (white brace). For the specific examples discussed in the article, the moiety Y would correspond to oxygen in calcite, CH_2COOH in malonic acid, and CH_2CH_2COOH in succinic acid, and Z would correspond to calcium ions in calcite or the second molecule in the unit cell for malonic and succinic acids.

of malonic and succinic acids is practically the same as the orientation of the carboxylic groups in SAMs.

Interestingly, on the basis of purely epitaxial considerations, one should expect that the preferred nucleating plane for malonic acid is likely to correspond to the $\{h0l\}$ family, where the distance between the molecules in the b direction ($b = 5.14$ Å) corresponds well to the unit cell dimension in the SAM ($a = 5$ Å) (Figure 3a). The nucleation of the malonic acid crystals from the (10-2) plane that belongs to the $\{h0l\}$ family will provide a better lattice match at the interface and will be more favorable than the orientational match with the second carboxylic group that will therefore be discriminated from the nucleation. Similarly, the preferred nucleating plane for the succinic acid is likely to correspond to the $\{hk0\}$ family, where the distance between the molecules in the c direction ($c = 5.10$ Å) corresponds well to the unit cell dimension in the SAM (Figure 3b). The nucleation of the succinic acid crystals from the (120) plane that belongs to the $\{hk0\}$ family will provide a better lattice match at the interface and will be more favorable than the orientational match with the carboxylic groups in the second molecule in the unit cell that will therefore be discriminated from the nucleation. This indicates that the discrimination between the different carboxylic groups in the crystal arises from the optimization of the lattice mismatch at the interface.[23]

The lattice mismatch at the interface might also explain the observed differences in the crystal coverage, crystal sizes, and densities of nucleation. For example, in the case of malonic acid on $HS(CH_2)_{11}CO_2H$, the coverage is much lower and the crystals are smaller than the crystals grown on $HS(CH_2)_{10}CO_2H$. This might be due to a higher lattice mismatch between the SAM template and the (10-2) plane as compared to the (01-1). We have previously demonstrated that a larger lattice mismatch between the SAM substrate and the nucleating plane of a templated crystal leads to the growth of smaller crystals.[23]

We can generalize and propose that the oriented functional groups in the monolayer may serve as surrogate moieties of the molecules or ions in the nucleating crystals, thus inducing the directional binding of the subsequent molecules at an angle dictated by the functional groups in the SAMs (Figure 4). If multiple functional groups or molecules in the crystal can

orient at the organic surface, then the system will select nucleating planes that provide minimal lattice mismatch. Such interfacial orientational alignment and discrimination of highly mismatched lattices ultimately result in fixed, well-controlled, oriented nucleation.

In conclusion, our results strongly suggest that the translation of stereochemical information through the interface is the common mechanism that governs the oriented growth of organic and inorganic crystals on SAMs. These findings are very important in the understanding of the underlying principles by which various organic surfaces—and most probably also biological templates—control the crystallization process. Because organic surfaces can be tailored to present various functional groups with finely tuned orientations, they may be used as potent crystallization templates that can induce nucleation and stabilization of a low-symmetry phase and its growth in an arbitrary crystallographic direction. A knowledge of the mechanisms of oriented crystallization and polymorph selectivity in such systems has essential implications, among other areas, in the pharmaceutical industry, where controlled crystallization of complex organic molecules often presents a critical difficulty.

Materials and Methods

Substrates. (110) Si wafers were coated with 1 nm of Ti as an adhesion promoter, followed by a 100 nm Au coating. An AJA sputtering system was used to prepare the coatings. The typical grain size of the gold was approximately 30 nm, and the mean roughness was 1 nm. Au films had an extremely strong (111) texture. We also used a bare piece of (110) Si wafer as a control template for crystal growth.

SAM Surface Preparation. $HS(CH_2)_{11}CO_2H$ and $HS(CH_2)_{10}CO_2H$ (chemical purity of 96%) were purchased from Sigma-Aldrich. SAMs of $HS(CH_2)_{11}CO_2H$ and $HS(CH_2)_{10}CO_2H$ were formed on gold substrates by exposing the surfaces to a 5 mM solution of thiol in absolute ethanol for 24 h, followed by extensive rinsing with ethanol.

Crystal Growth. Malonic acid ($HOOCCH_2COOH$) and succinic acid ($HOOCCH_2CH_2COOH$) were purchased from Sigma-Aldrich. Stock solutions of 0.125 M in water were prepared for both acids, and a few drops were placed on the substrates and allowed to evaporate in air. Once the solution attained its solubility limit, crystals were formed on the surfaces. All crystallization experiments were carried out at room temperature (25° ± 2 °C) over a range of humidity of 20−30%.

Characterization. The characterization of the crystals formed on the SAM surfaces was undertaken first on a Leica DMRX optical microscope, followed by X-ray diffraction (XRD) on a D8 Bruker diffractometer. Samples were further imaged with a JEOL JSM-6390LV SEM. For this purpose, samples were coated with 5 nm of Pt/Pd by sputtering. Imaging was carried out at an acceleration voltage of 10−15 keV.

Supporting Information Available: Powder X-ray diffraction spectra of succinic (A) and malonic (B) acids grown on a bare Si(110) wafer as a control experiment. Schematic presentation of a rocking curve experiment showing the origin of the possible errors in the determination of the nucleating planes on the basis of the XRD data. This material is available free of charge via the Internet at http://pubs.acs.org.